Supporting information to:

Metagenomic and metatranscriptomic characterization of syntrophic propionate- and butyrate-oxidizing bacterial communities in Qiangyong proglacial lake sediments on the Tibetan Plateau

Rong Wen et al.

***Correspondence author**

Pengfei Liu, (liupf@lzu.edu.cn)

This PDF file includes:

Supplementary Methods

Supplementary Figs. 1-9

Titles for the Supplementary Tables:

Table S1 Physicochemical properties of QY proglacial lake sediments in January and May.

Table S2 Taxonomic classification of reported syntrophic propionate- and butyrate-oxidizing bacteria (SPOB/SBOB) at genus level.

Table S3 Taxonomic affiliations of zOTUs associated with putative syntrophic propionate- and butyrate-oxidizing bacteria at genus level.

Table S4 Network parameters of co-occurrence analysis for syntrophic and non-syntrophic bacterial zOTUs.

Table S5 Taxonomic classification and genomic features of the 1,336 non-redundant metagenome-assembled genomes (MAGs) derived from QY sediment samples.

Table S6 Key enzymatic steps, KO identifiers, and reactions of the methylmalonyl-CoA (MMC) pathway for syntrophic propionate oxidation.

Table S7 Key enzymatic steps, KO identifiers, and reactions of the β-oxidation pathway for syntrophic butyrate oxidation.

Table S8 Genomic characteristics of 23 putative syntrophic bacteria (19 SPOB and 4 SBOB) identified from QY proglacial lake sediments MAGs.

Table S9 Taxonomic classification and genomic features of the 315 non-redundant metagenome-assembled genomes (MAGs) derived from NCBI RefSeq database.

Table S10 Genomic characteristics of 135 putative syntrophic bacteria (39 SPOB and 96 SBOB) identified from NCBI RefSeq database.

Table S11 POCP-based classification of 23 SPOB genera and their representative MAGs.

Table S12 POCP-based classification of 5 SBOB genera and their representative MAGs.

Table S13 Hydrogenase ([NiFe] and [FeFe]) distribution in representative genomes of 23 syntrophic propionate-oxidizing bacterial (SPOB) genera.

Table S14 Hydrogenase ([NiFe] and [FeFe]) distribution in representative genomes of 5 syntrophic butyrate-oxidizing bacterial (SBOB) genera.

Table S15 Formate dehydrogenases distribution in representative genomes of 23 syntrophic propionate-oxidizing bacterial (SPOB) genera.

Table S16 Formate dehydrogenases distribution in representative genomes of 5 syntrophic butyrate-oxidizing bacterial (SBOB) genera.

Table S17 Environmental sources of RefSeq genomes related to novel SPOB/SBOB lineages from QYPL sediments.

Other supporting materials for this manuscript include the following:

MAGs and annotation of all putative SPOB and SBOB, Supplementary Tables S1-S17 are available at figshare https://figshare.com/articles/dataset/QY_syntrophic_bacterial/29345711. Specifically, the link for Supplementary Tables S1-S17 is https://figshare.com/articles/dataset/QY_syntrophic_bacterial/29345711?file=55454384.

Supplementary Methods

Curation of SPOB and SBOB related MAGs

The presence of key enzymes involved in the methylmalonyl-CoA (MMC) pathway and the beta-oxidaiton pathway were used to curate SPOB and SBOB, respectively. The MMC pathway for propionate oxidation proceeds through 11 sequential enzymatic steps: (1) propionate activation to propionyl-CoA, catalyzed by propionate-CoA transferase/acetate-CoA ligase (K00625, K00925, K01026, K01895, K01905, K01908, K13788, K15024, K22224); (2) carboxylation to (S)-methylmalonyl-CoA by methylmalonyl-CoA carboxyltransferase (K01965, K01966, K03416, K11263, K15036, K17489, K17490, K19312, K01604); (3) epimerization to (R)-methylmalonyl-CoA via methylmalonyl-CoA epimerase (K05606); (4) isomerization to succinyl-CoA by methylmalonyl-CoA mutase (K01847, K01848, K01849); (5) conversion of succinyl-CoA to succinate via succinyl-CoA synthetase (K01902, K01903); (6) oxidation of succinate to fumarate by succinate dehydrogenase (K00234, K00235, K00236, K00237, K00239, K00240, K00241, K00242, K00244, K00245, K00246, K00247, K18859, K18860); (7) hydration of fumarate to malate by fumarate hydratase (K01675, K01676, K01677, K01678, K01679, K01774); (8) dehydrogenation of malate to oxaloacetate by malate dehydrogenase (K00024, K00025, K00026); (9) decarboxylation of oxaloacetate to pyruvate via pyruvate carboxylase (K01958, K01959, K01960, K01006, K01007); (10) oxidative decarboxylation of pyruvate to acetyl-CoA by pyruvate ferredoxin oxidoreductase (K03737, K00169, K00170, K00171, K00172, K00189); and (11) acetate formation from acetyl-CoA via acetate-CoA ligase (K01895, K01905, K22224). This pathway enables syntrophic propionate oxidizers to couple propionate degradation with energy conservation, with key redox steps including succinate to fumarate, malate to oxaloacetate, and pyruvate to acetyl-CoA (Table S6).

The butyrate oxidation pathway in syntrophic bacteria proceeds through seven key enzymatic steps, each catalyzed by specific enzymes with corresponding KO identifiers (Table S7): (1) butyrate activation to butyryl-CoA by CoA transferase (K00634, K00929, K01034, K01035); (2) oxidation of butyryl-CoA to crotonyl-CoA via acyl-CoA dehydrogenase (K00248); (3) hydration of crotonyl-CoA to 3-hydroxybutyryl-CoA by enoyl-CoA hydratase (K01692, K01715, K01782, K17865); (4) oxidation to acetoacetyl-CoA by 3-hydroxybutyryl-CoA dehydrogenase (K00023, K00074, K07516); (5) cleavage to two acetyl-CoA via acetyl-CoA acetyltransferase (K00626); (6) conversion of acetyl-CoA to acetylphosphate by phosphotransacetylase (K00625); and (7) ATP generation through acetate formation via acetate kinase (K00925).

To remove aerobes that using propionate or butyrate, we further removed MAGs encoding terminal oxidoreductases (K00404-K00407, K02274-K02277, K02297-K02300, K02826-K02829, K15408, K15862, K22501).

Anaerobic incubation of proglacial sediment

Anaerobic microcosm incubations of sediments (1:2 sediment:water ratio) from Site 1 (January) of Qiangyong proglacial lake were conducted at 15°C for 150 days in the dark without shaking under four treatment conditions: (1) 40 mM propionate, (2) 40 mM butyrate, (3) 0.5% (w/w) cellulose–hemicellulose mixture (1:1), and (4) 0.5% (w/w) cellulose–hemicellulose mixture (1:1) amended with 10 mM Sodium 2-

bromoethanesulfonate (BES, a specific inhibitor of methanogens). Propionate and butyrate were added to test if they could be degraded and linked to methane production by sediment microbiota. Cellulose-hemicellulose mixtures (1:1) with and without 10 mM BES were set up to test whether intermediates (propionate and butyrate) could be produced and subsequently consumed by sediment microbiota.

Gas samples were periodically collected from the headspace of the tubes using a gas-tight pressure-lock syringe (Dynatech), with sampling intervals ranging from 10–20 days. Methane concentrations were measured using an Agilent 8890 gas chromatograph system equipped with a flame ionization detector, following separation on a HayeSep Q column (2.44 m length, 2 mm diameter) with pure H_2 and pure N_2 as carrier gases. During the incubation, liquid samples were taken with an anaerobically pre-treated syringe and then centrifuged at 12,000 × g for 2 mins to remove particles. The supernatants were filtered through 0.22 μm membrane filters (Sangon Biotech, China). Volatile fatty acid (VFA) concentrations (acetate, propionate, butyrate) were determined by high-performance liquid chromatography (LC-2030 Plus, Shimadzu) equipped with a C18 reverse-phase column (4.6 × 250 mm, 5 μm particle size). Analysis conditions were: UV detection at 210 nm, 10 μL injection volume, isocratic elution with 1% (v/v) acetonitrile in 99% (v/v) 20 mM NaH_2PO_4 (pH 2.0 adjusted with H_3PO_4) mobile phase at 1.0 mL/min flow rate. The production of methane and consumption/accumulation of propionate and butyrate are shown in Fig. S9.

Supplementary Figures

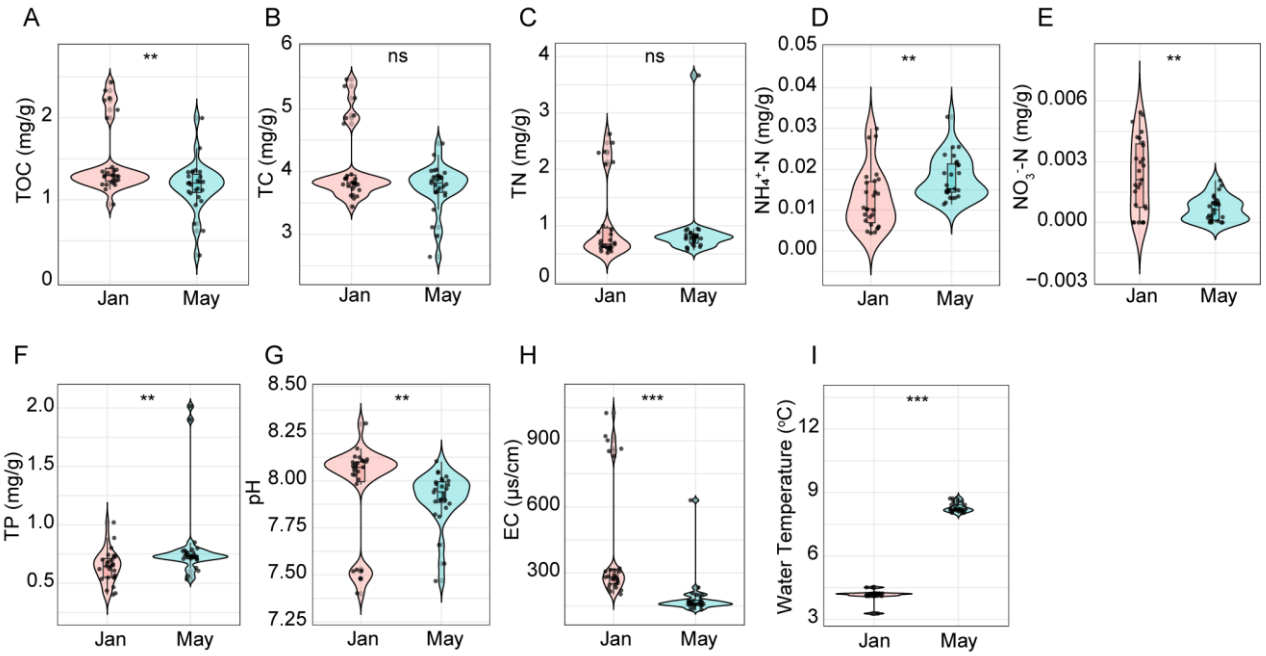

Fig. S1 Comparison of physicochemical properties of QY proglacial lake sediments between January and May. (A) Total organic carbon content, (B) Total carbon content, (C) Total nitrogen content, (D) Ammonium nitrogen content, (E) Nitrate nitrogen content, (F) Total phosphorus content, (G) pH value, (H) Conductivity, (I) Water Temperature. Mann-Whitney U test P<0.001, ***; P<0.01, **; P<0.05, *. Groups labeled with 'ns' indicate no significant differences between them.

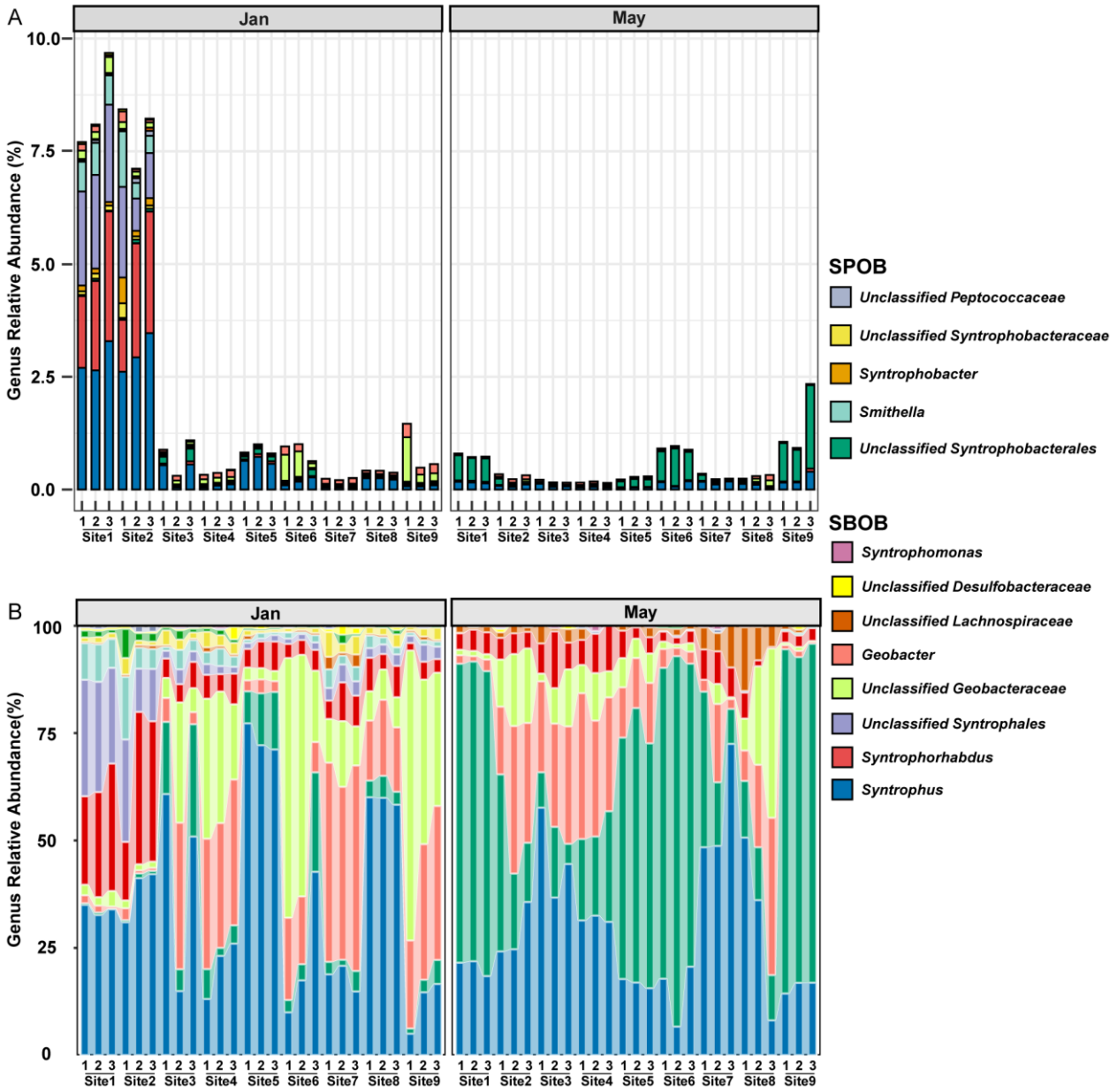

Fig. S2 Stack bar plot showing the relative abundance of syntrophic bacteria. (A) Relative abundance of syntrophic bacteria within the total bacteria communities. (B) Relative composition of syntrophic bacteria, with the abundance of all syntrophic bacteria scale up to 100%.

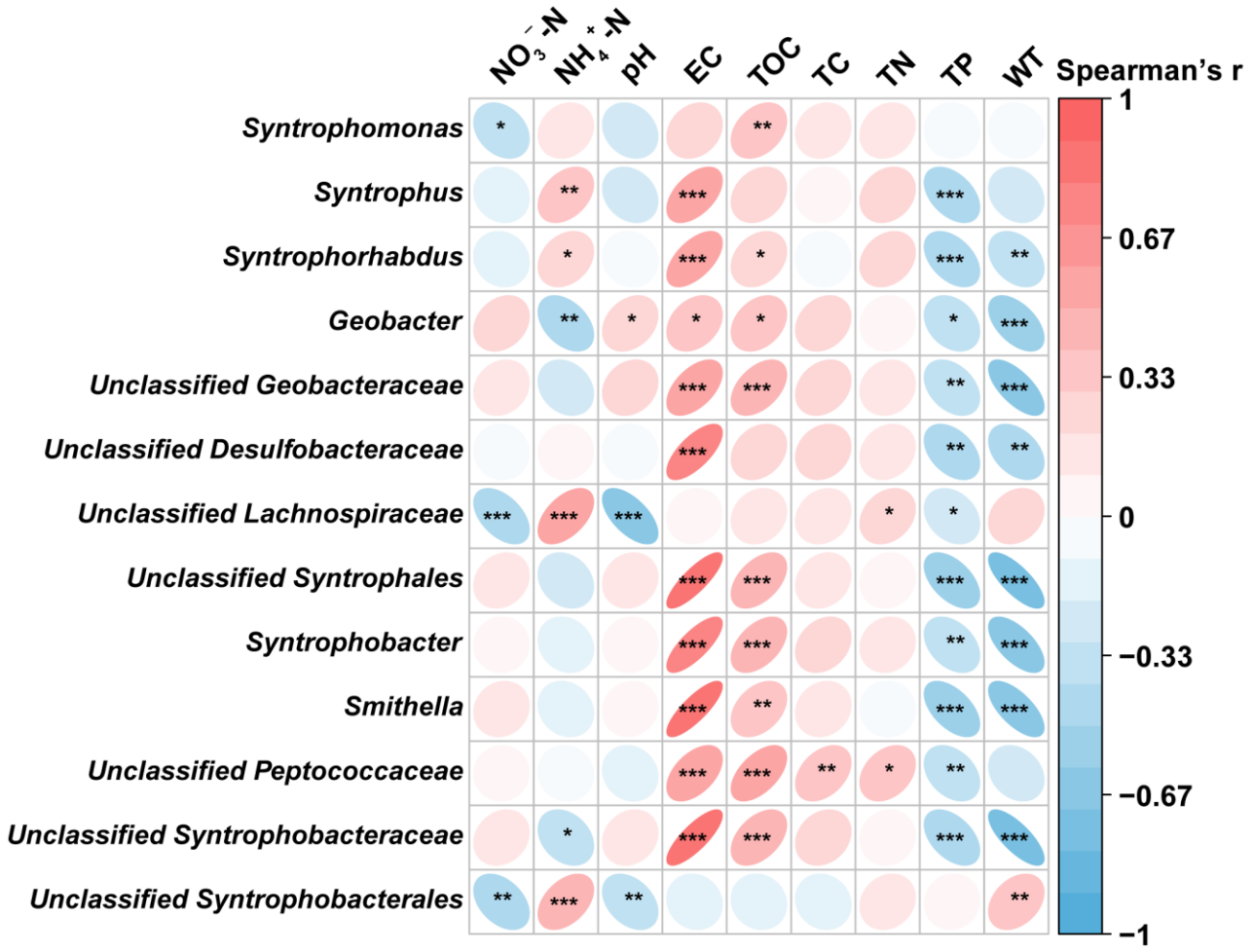

Fig. S3 Spearman correlation analysis between syntrophic bacterial genera and physicochemical properties in QY proglacial lake sediments. The heatmap displays correlations between the relative abundance of 13 syntrophic bacterial genera (8 propionate-oxidizing and 5 butyrate-oxidizing syntrophic bacteria) and 9 sediment physicochemical parameters (nitrate nitrogen, ammonium nitrogen, pH, conductivity, total organic carbon, total carbon, total nitrogen, total phosphorus, water temperature). Ellipse colors represent correlation direction (red: positive; blue: negative) and sizes indicate strength. Significant correlations are marked: *P < 0.05, **P < 0.01, ***P < 0.001.

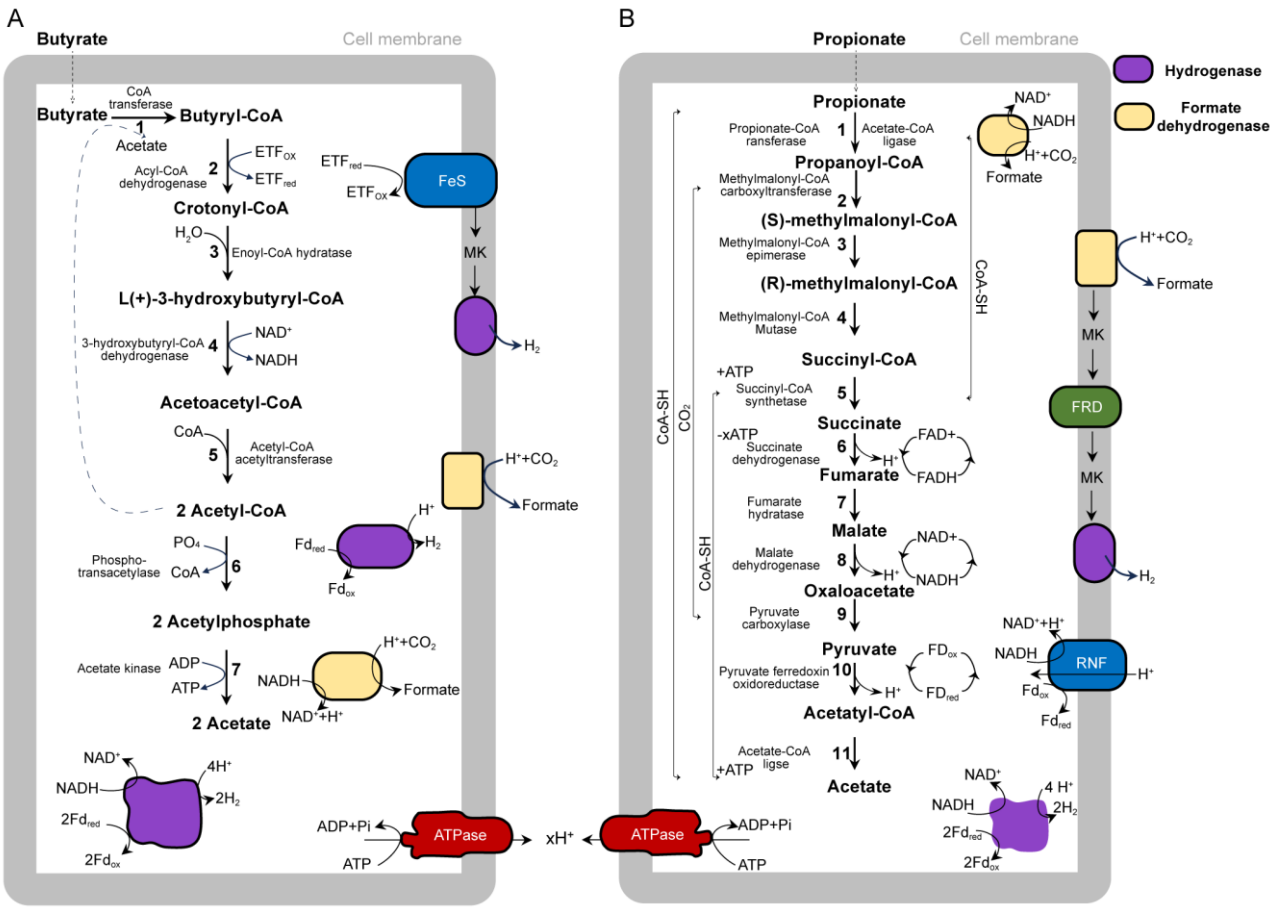

Fig. S4 Metabolic pathways of syntrophic butyrate and propionate oxidation in anaerobic bacteria. Panel A shows the β-oxidation pathway for butyrate degradation through seven enzymatic conversions to acetate. Panel B displays the methylmalonyl-CoA pathway for propionate oxidation, comprising eleven enzymatic steps from propionate activation to oxaloacetate formation, with subsequent decarboxylation yielding acetate as the end product. Each enzymatic step is annotated with its corresponding KEGG Orthology (KO) identifier. The butyrate pathway (Panel A) involves: (1) butyrate activation (K00634, K00929, K01034, K01035), (2) butyryl-CoA oxidation (K00248), (3) crotonyl-CoA hydration (K01692, K01715, K01782, K17865), (4) 3-hydroxybutyryl-CoA oxidation (K00023, K00074, K07516), (5) acetoacetyl-CoA cleavage (K00626), (6) acetyl-CoA conversion (K00625), and (7) acetate formation (K00925). The propionate pathway (Panel B) includes: (1) propionate activation (K00625, K00925, K01026, K01895, K01905, K01908, K13788, K15024, K22224), (2) carboxylation (K01965, K01966, K03416, K11263, K15036, K17489, K17490, K19312, K01604), (3) epimerization (K05606), (4) isomerization (K01847-K01849), (5) succinyl-CoA conversion (K01902, K01903), (6) succinate oxidation (K00234-K00237, K00239-K00242, K00244-K00247, K18859, K18860), (7) fumarate hydration (K01675-K01679, K01774), (8) malate dehydrogenation (K00024-K00026), (9) oxaloacetate decarboxylation (K01958-K01960, K01006, K01007), (10) pyruvate oxidation (K03737, K00169-K00172, K00189), and (11) acetate synthesis (K01895, K01905, K22224). Key enzymes involved in interspecies electron transfer, including hydrogenases and formate dehydrogenases, are functionally associated with this pathway. The pathway reconstructions were based on genomic annotations from metagenome-

assembled genomes of syntrophic bacteria, with enzymatic reactions verified through KEGG database comparisons. Pathway details in Panel A correlate with Fig. 5 and Supplementary Table S7, while Panel B corresponds to Fig. 4 and Supplementary Table S6.

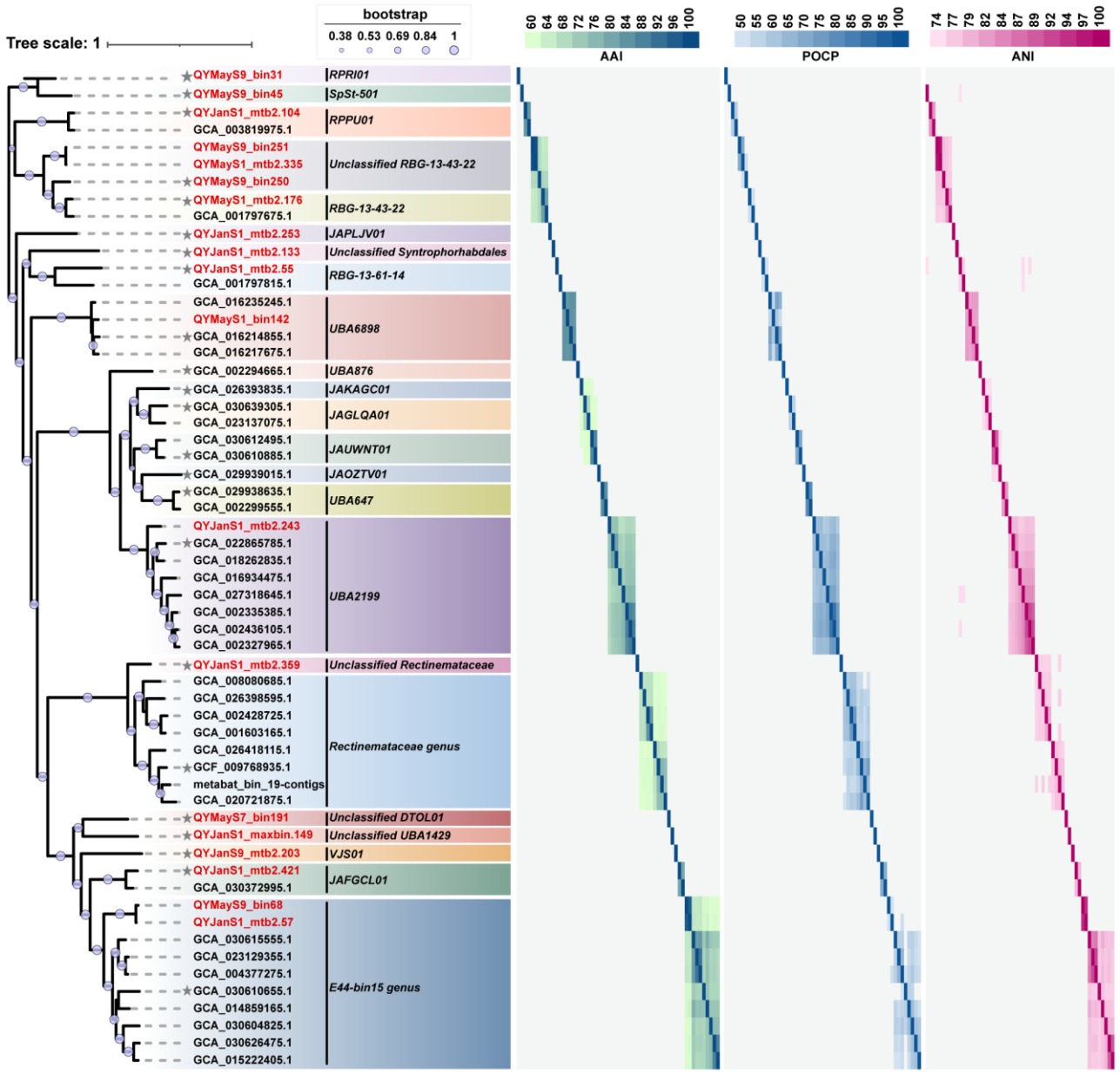

Fig. S5 Similarity of MAGs with syntrophic propionate oxidation potentials. Average Amino Acid Identity (AAI), Percentage of Conserved Proteins (POCP), and Average Nucleotide Identity (ANI) analyses were conducted on 58 dereplicated genomes.

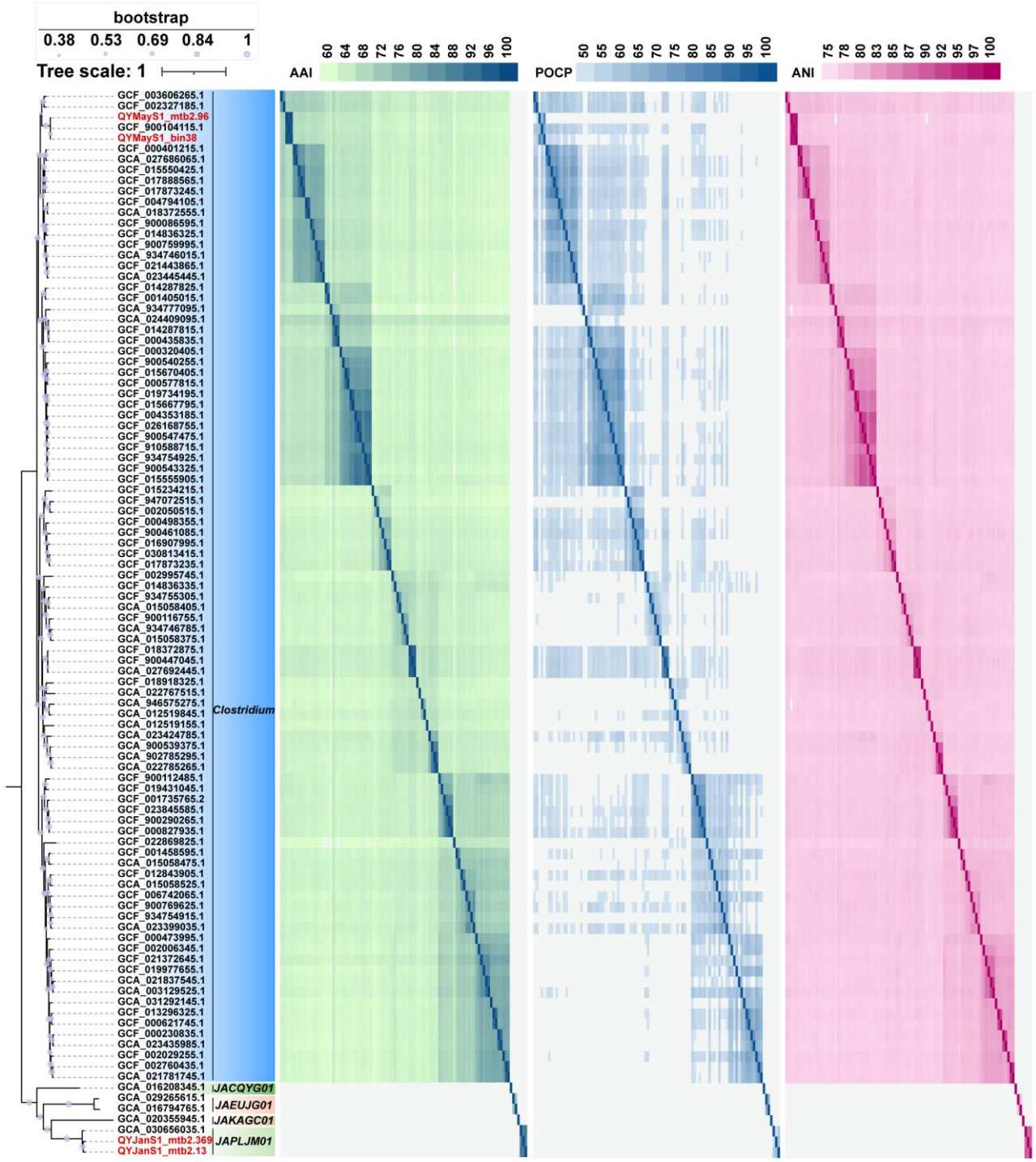

Fig. S6 Similarity of MAGs with syntrophic butyrate oxidation potentials. Average Amino Acid Identity (AAI), Percentage of Conserved Proteins (POCP), and Average Nucleotide Identity (ANI) analyses were conducted on 100 dereplicated genomes.

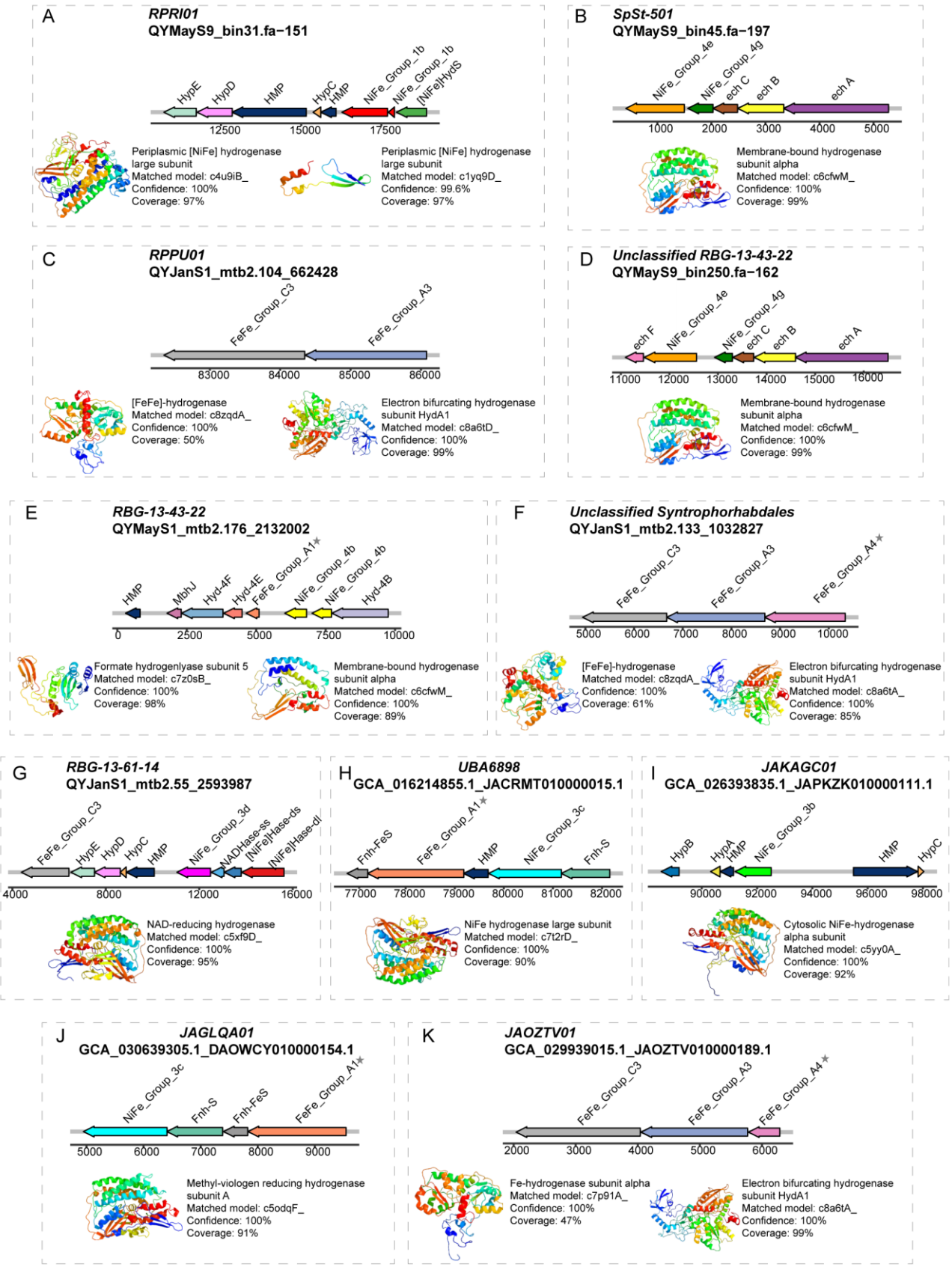

Fig. S7 Genomic organization and structural modeling of hydrogenases in representative syntrophic bacterial lineages. (A-S) Representative genomes of syntrophic propionate-oxidizing bacterial genera showing gene cluster arrangements (top) and predicted hydrogenase structures (bottom). (T-V) Representative

genomes of syntrophic butyrate-oxidizing bacterial genera with corresponding gene clusters and structural models. All genomes represent the most complete and least contaminated MAGs in each genus. Structural predictions were modeled with > 99% confidence using Phyre2.2.

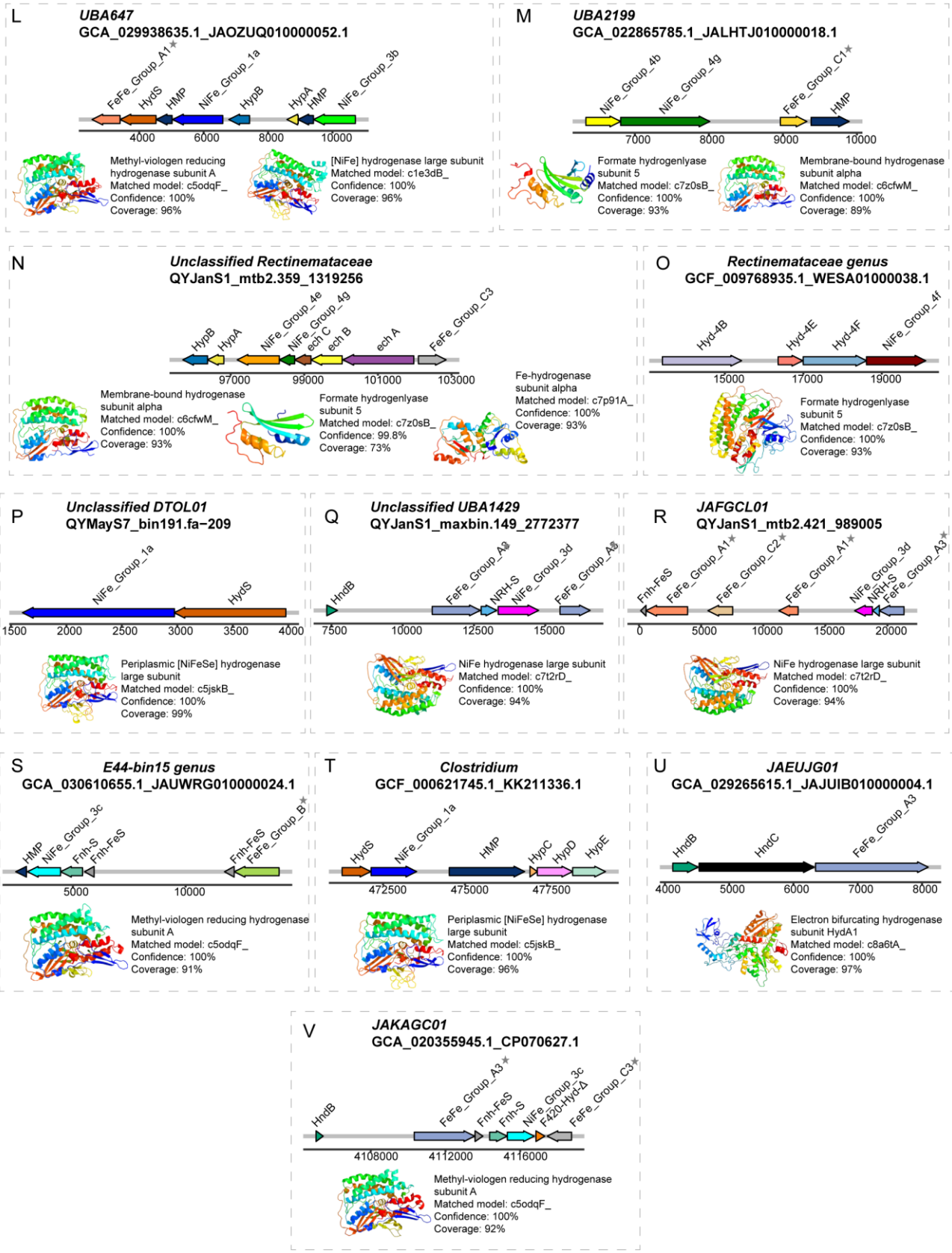

Fig. S7 Continue.

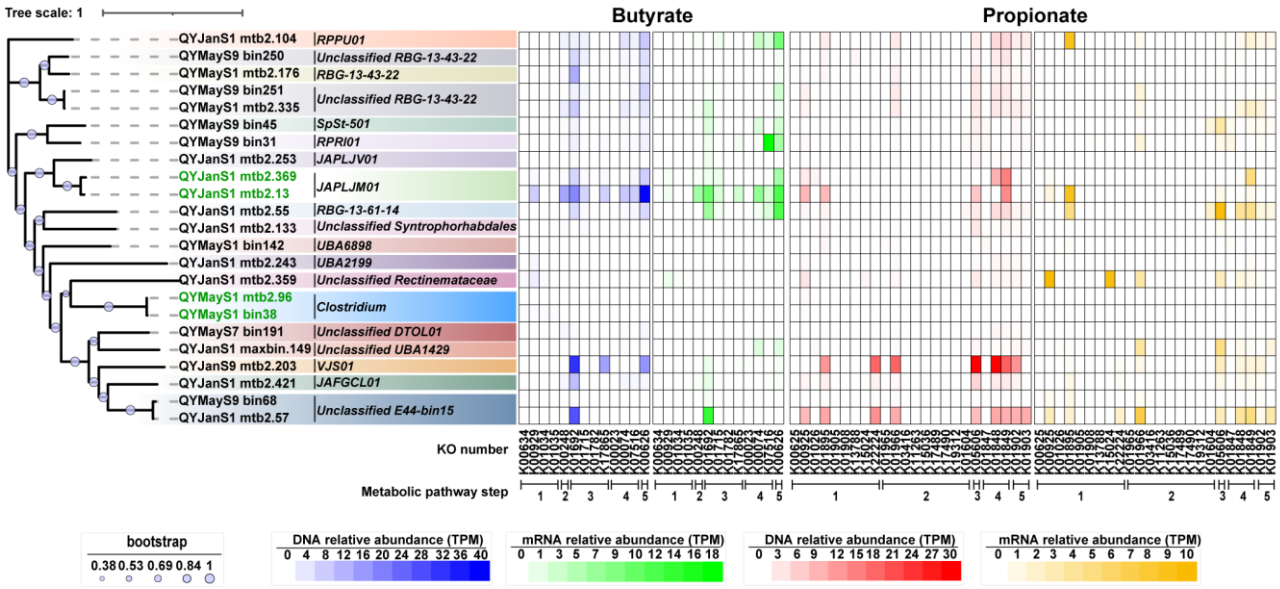

Fig. S8 Key gene abundance and transcriptional activity of syntrophic bacteria in QY proglacial lake sediment. Maximum abundance of key genes from each MAG at DNA (left) and mRNA (right) levels among the six samples, showing the first five steps of both methylmalonyl-CoA (MMC) and β-oxidation pathways.

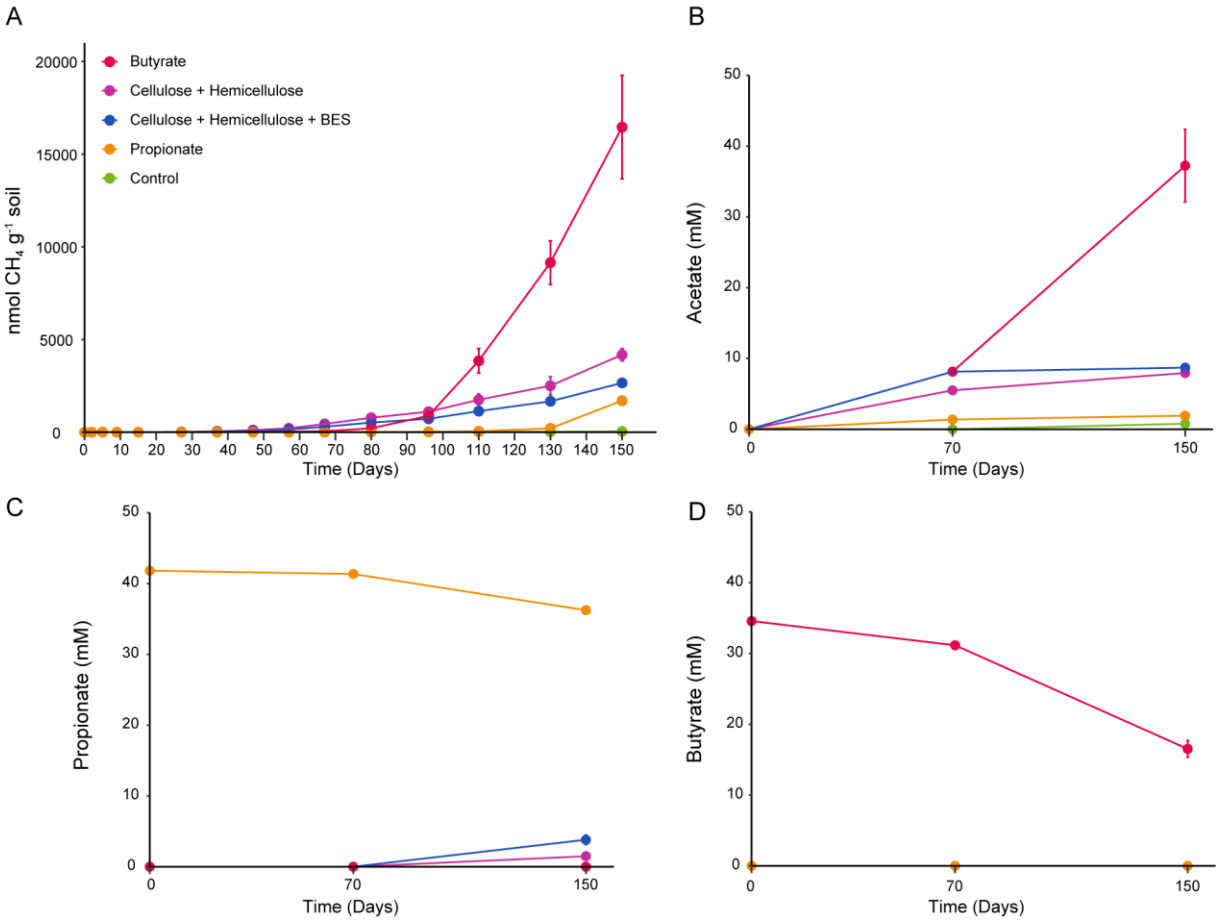

178

179 **Fig. S9 Degradation of propionate and butyrate linked to methane production in proglacial lake**
180 **sediments.** Anaerobic microcosm incubation of sediments (1:2 sediment:water ratio) from site 1 (January) of
181 Qiangyong proglacial lake at 15°C for 150 days under four treatment conditions: (1) 40 mM propionate, (2)
182 40 mM butyrate, (3) 0.5% (w/w) cellulose+hemicellulose mixture (1:1), and (4) 0.5% (w/w)
183 cellulose+hemicellulose mixture (1:1) with 10 mM BES. (A) Methane concentration over time, (B) Acetate
184 concentration over time, (C) Propionate concentration over time, and (D) Butyrate concentration over time.
185 Error bars represent the standard deviation of three biological replicates.